IIETA International Information and Engineering Technology Association
Advancing the World of Information and Engineering

Annales de Chimie - Science des Matériaux
Vol. 44, No. 4, August, 2020, pp. 231-238
Journal homepage: http://iieta.org/journals/acsm

Numerical Simulation of Water as Base Fluid Dispersed by Al_2O_3 Aluminum Oxide Nano-Sized Solid Particles with Various Concentrations

Chafika Zidani[1*], Rachid Maouedj[2], Mohamed Salmi[3,4]

[1] Unit of Research on Materials and Renewable Energies, Department of Physics, Faculty of Sciences, Abou Bekr Belkaid University, P.O. Box 119-13000-Tlemcen, Algeria
[2] Unité de Recherche en Energies Renouvelables en Milieu Saharien, URERMS, Centre de Développement des Energies Renouvelables, CDER, 01000, Adrar, Algeria
[3] Department of Physics, University of M'sila, B.P. 1713, M'sila 28000, Algeria
[4] Laboratory of Physics and Chemistry of Materials, University of M'sila, M'sila 28000, Algeria

Corresponding Author Email: chafikazidani@gmail.com

https://doi.org/10.18280/acsm.440401

Received: 2 June 2020
Accepted: 31 July 2020

Keywords:
characterization of nanofluids, physical properties, mechanical properties, fluid dynamics, turbulent viscosity, aluminum oxide, numerical simulation

ABSTRACT

Curves of pressure, lines of current, speed of fluid, fields and diagrams of kinetic energy, and plots of viscosity through a H_2O/Al_2O_3 nanofluid-heat exchanger with recirculation promoters are studied by using a computational approach and a two-dimensional algorithm. The simulation used four nanofluid fractions, i.e. ϕ = 0.5, 1, 2 and 4 percent, with four flow rates, i.e. *Re* = 5, 10, 15 and 20 ($\times 10^3$). Both the discontinuous-type deflectors and the detached-model bars are considered to reinforce the nanofluid field structure. The discontinuous-situation of these deflectors allows reducing the pressure on its front-corner by passing the fluid between their internal surfaces. In addition, the field is detached from the front-sharp-edge, forcing the creation of recycling-rings on their back-areas. While, the presence of the detached-bar model in both the top and the lower stations of the exchanger allows an improvement in the flow disturbance across the gaps through their interior-surfaces, and the formation of new recycling-cells near their right-sides. These vortices constitute opposite-currents where their strength increases with increasing nanofluid concentration and Reynolds values.

1. INTRODUCTION

Important review studies of transport characteristics of mass and heat of nanofluids have been addressed by many authors (Ozerinc et al. [1], M'hamed et al. [2], Liang and Mudawar [3], Kakaç and Pramuanjaroenkij [4], Zayed et al. [5], Estellé et al. [6], Farhana et al. [7], Ahmad et al. [8], Akilu et al. [9] and Menni et al. [10]). Minakov et al. [11] used H_2O-ZrO_2 nanofluids and experimental models to enhance the convective turbulent structure in channels and tubes with no promoters. Mohebbi et al. [12] used the LB (Lattice-Boltzmann) approach to simulate the convective-heat-transfer of nanofluids in an extended surfaces' channel under many solid-fractions, flow rates, and obstacles' sizes. Selimefendigil and Öztop [13] reported analyses of convective-transfer simulations of nanofluids in a branching-duct with annulus. Xu and Cui [14] investigated the case of a fully-developed flow in the mixed-convection through a duct filled with porous-type mediums. Ameri and Eshaghi [15] improved the laminar performance of a porous-media flat-plate collector by using Fe_3O_4-nanofluid flows. Edalatpour and Solano [16] conducted investigations on different heat-transport parameters in a 3D flat-plate collector. Laminar H_2O-Al_2O_3 nanofluid fields under various Al_2O_3 solid fractions were considered. Tomy et al. [17] studied the improvement of transport of heat in a flat-plate solar-collector by using the MATLAB. They confirmed the thermal performance in terms of exit-station temperature, coefficient of heat transport, and the efficiency by experimental validation. Anbuchezhian et al. [18] analyzed the case of nanofluids in laminar flows for solar applications. Anbuchezhian et al. [19] studied the MHD convective filed and thermal transport of an incompressible-model and viscous-type nanofluid through a porous media by using theoretical techniques. Using BBD (Box-Behnken-design) code, Ghorbanian et al. [20] physically optimized a corrugated-surface and porous-type cavity by nanofluid flows in the solar-radiation case. Khamis et al. [21] used the approximations of boundary-layer and Boussinesq as well as the model of Buongiorno nanofluid to simulate unsteady-type flows of H_2O-Cu and H_2O-Al_2O_3 nanofluids with variable-viscosity inside a porous-type duct with buoyancy-force. Meibodi et al. [22] theoretically studied the H_2O-SiO_2/EG performance in solar collectors by using experimental results. Khullar and Tyagi [23] investigated the importance of nanofluids in a solar-concentration system for water heating. Matin and Hosseini [24] reported analytical studies as well as numerical investigations on the nanofluid transport over an inclined-type transparent-model plate in a porous-type medium. Menni et al. [25, 26] used both the nanofluids and the vortex promoters to rise the performance of rectangular-duct heat exchangers, under the steady-turbulent conditions.

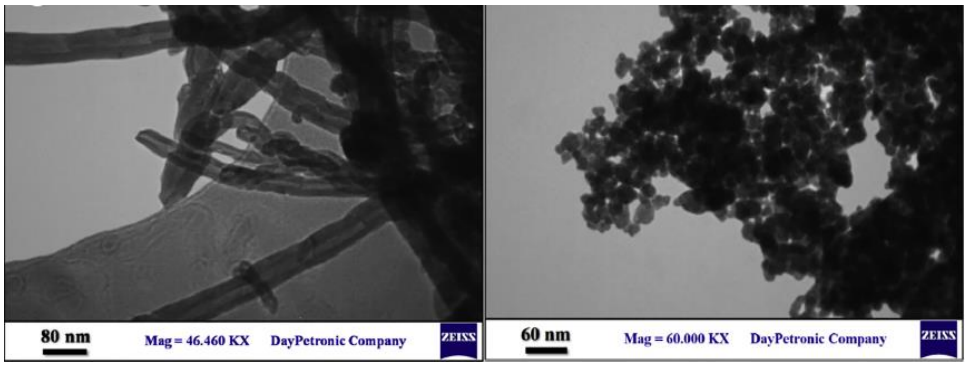

(a) MWCNT (TEM-image) [27] **(b)** Fe_2O_3 (TEM-image) [27]

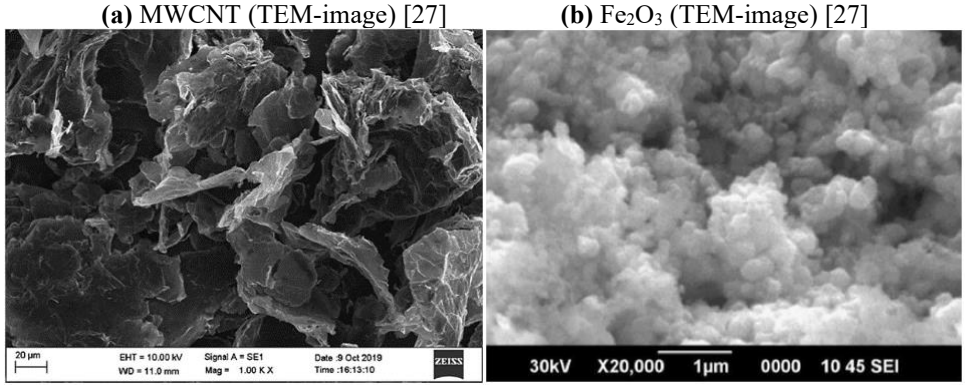

(c) Graphene (SEM-image) [28] **(d)** Al_2O_3/Cu (SEM-image) [29, 30]

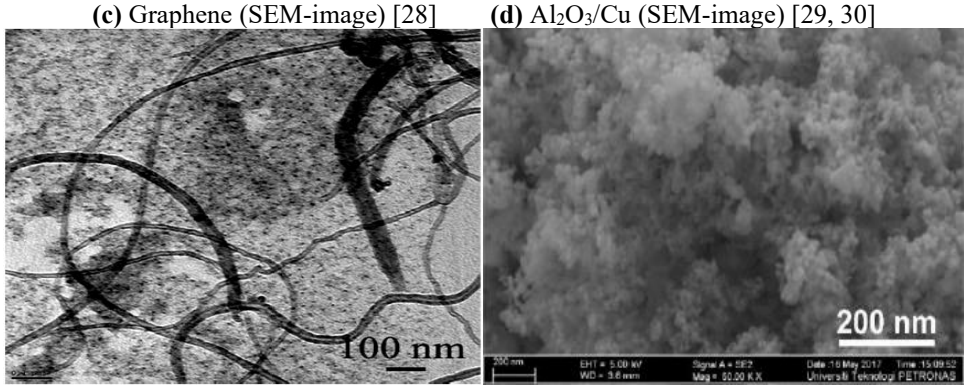

(e) Ag-(MWNT-HEG) (TEM-image) [31] **(f)** Titania (SEM-image) [32]

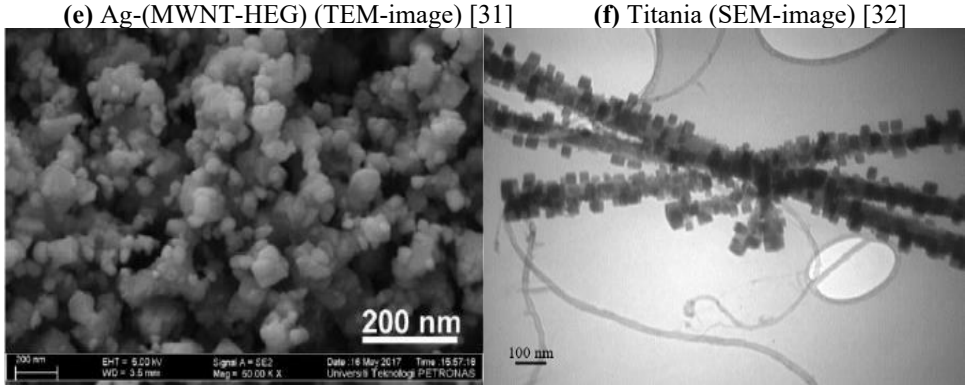

(g) CuO/C (SEM-image) [32] **(h)** Fe_2O_3-CNT (TEM-image) [33]

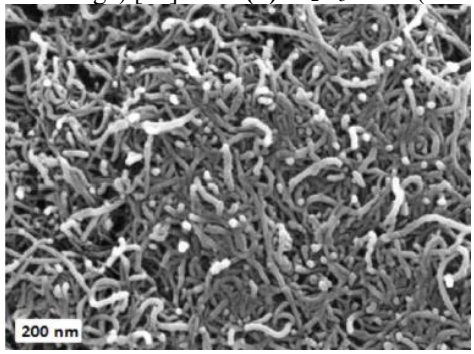

(i) SWCNTs (SEM-image) [34]

Figure 1. Various images of solid nano-particles used in previous nanofluid studies

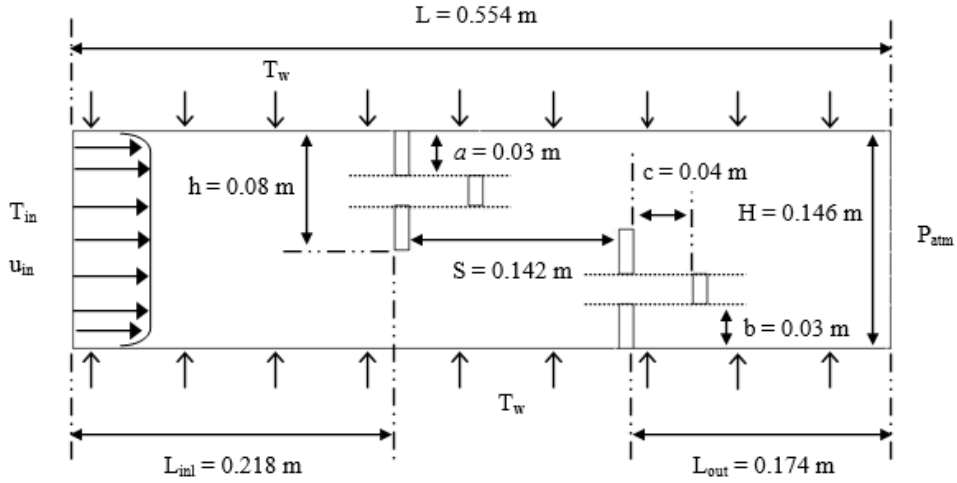

Figure 2. Numerical-domain

Also, excellent characterizations of solid nanoparticles (Figure 1) have been studied by many authors (Asadikia et al. [27], Balaji et al. [28], Suresh et al. [29, 30], Baby and Sundara [31], Akilu et al. [32], Aghabozorg et al. [33] and Terrones [34]). All these solid particles are presented for preparing nanofluids.

In this numerical simulation, a nanofluid of H_2O-Al_2O_3 with 0.5, 1, 2 and 4 percent fractions, is presented as fluid of transport of heat inside a 2D rectangular-duct heat-exchanger. The duct has two types of vortex promoters, i.e. discontinuous-type deflectors and detached-model bars, to reinforce the turbulent nanofluid field structure. The finite volume and SIMPLE approaches are used for calculation and a variable flow-rate, *Re*, [5×10^3 to 2×10^4] is applied to reinforce the turbulence.

2. PHYSICAL MODEL

2.1 Case study

The study proposes a new structure for a simple finned air-heat exchanger [35] by introducing new vortex promotors, namely, intermittent deflectors, rather than straight baffles. A 2nd model of promoters has been added, namely, disconnected bars (Figure 2). The combination of the two promoter models enables improved dynamic performance in order to improve heat transfer.

All engineering data were selected from the experience of Demartini and his colleagues [35] received for a rectangular-duct air-heat exchanger consisting of simple promoters within disconnected bars.

2.2 Al_2O_3-H_2O nanofluid

In addition to the developed promoter technique, a nanofluid is used as an alternative to conventional fluid (air) to further enhance the heat transfer. The proposed fluid is the conventional liquid (water) dispersed with nanometer solid particles of Al_2O_3 (aluminum hydroxide) according to a variable concentration from 0.5 to 4 percent.

Mathematically, the various physical properties of the developed fluid can be determined using the equations shown by Pourfattah et al. [36].

3. NUMERICAL MODEL

3.1 Limit conditions

Four boundary conditions are adopted in the simulation, namely, the regular inlet speed ($u = 0$ and $v = 0$) with an outlet subject to P_{atm} (atmospheric pressure) [35], as well as, both of the two horizontal axes of the exchanger are hot at a constant temperature (of 375 K) [37], while the solid walls are subject to the non-slip-and-impermeability-boundary conditions [35].

3.2 Resolution methods

The mathematical equations describing the turbulent flow, i.e. mass and momentum conservations, are solved using the finite-volume technique [38] and the SIMPLE [38] algorithm. The standard model of *k*-epsilon [39] is used to model the turbulent field structure. This model has proven its effectiveness in many studies received for baffled heat exchangers, as stated in the numerical study of Chamkha et al. [40] who compared (i.e. validation) the considered model with other models as well as with the experimental results reported by Demartini et al. [35]. The comparison showed the existence of quantitative and qualitative convergence between the standard model and Demartini's experimental data under the same conditions.

4. RESULTS AND DISCUSSIONS

4.1 Pd field

The presence of intermittent deflectors and disconnected bars inside the exchanger has a significant effect on the Pd (dynamic pressure) values. There are high values across the gaps between the interior faces of each deflector, as well as near the front-sharp-edges of each bar. The most stressed regions are those areas adjacent to the upper faces of the deflector, especially near the top exchanger wall (Figure 3).

In addition, there is a direct correlation between the Pd values and Re number with ϕ (Al_2O_3 particle volume concentration), as shown in Figure 4.

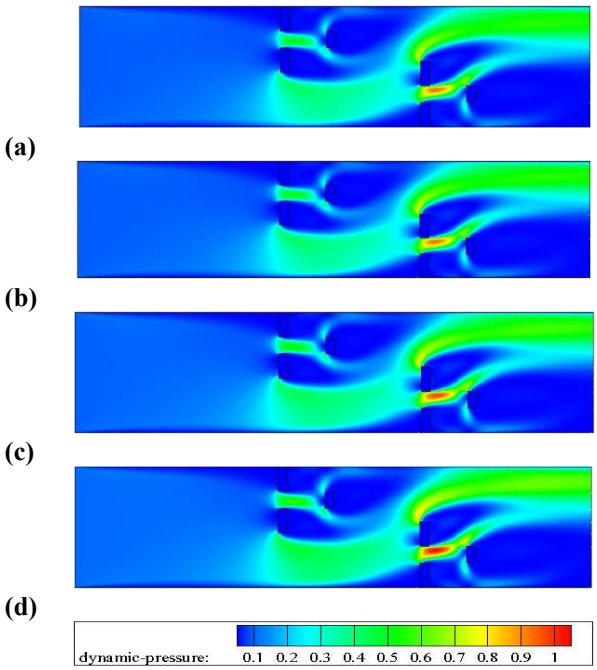

Figure 3. Pd field (in Pa) field for ϕ = (a) 0.5%, (b) 1%, (c) 2%, and (d) 4%, $Re = 50\times10^2$

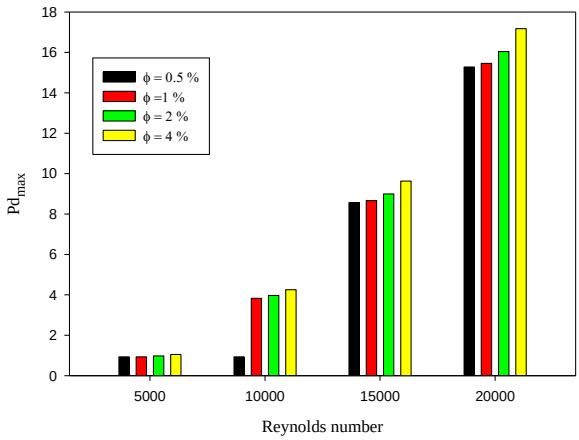

Figure 4. Pd_{max} for various Re numbers and ϕ concentrations

4.2 Ψ field

As expected, the nanofluid-flow is disturbed due to the presence of these deflectors inside the exchanger, as shown in Figure 5. The Al_2O_3-H_2O current flows from the inlet and then disturbs as the nanofluid approaches the first intermittent deflector. As a result of the presence of this promoter, a part of the current is stagnated on its upper-left-side. Another part of the current crosses the gap between the upper and lower sections of the same promoter, while the majority of the flow deviates towards the bottom of the deflector.

The intermittent configuration of this promoter allows reducing the Pd on its front corner by passing the current between their internal-surfaces. In addition, the flow is detached from the front-sharp-edge of the promoter, forcing the creation of recycling-rings on their back-areas.

The same structure is presented next to the second intermittent deflectors by forming the recirculation zones in their left and right faces. While, the presence of the disconnected bars in the upper and lower stations of the exchanger allows an increase in the nanofluid disturbance across the gaps through their interior-surfaces, and the formation of new recycling-cells near their right-sides. As shown in Figure 5, the strength of these vortices is increased by enhancing the nanofluid flow in larger quantities in terms of the particles of Al_2O_3 aluminum oxide. The result analysis also shows that the recirculation regions' intensity augments with increasing of flow rate in terms of Re number (Figure 6).

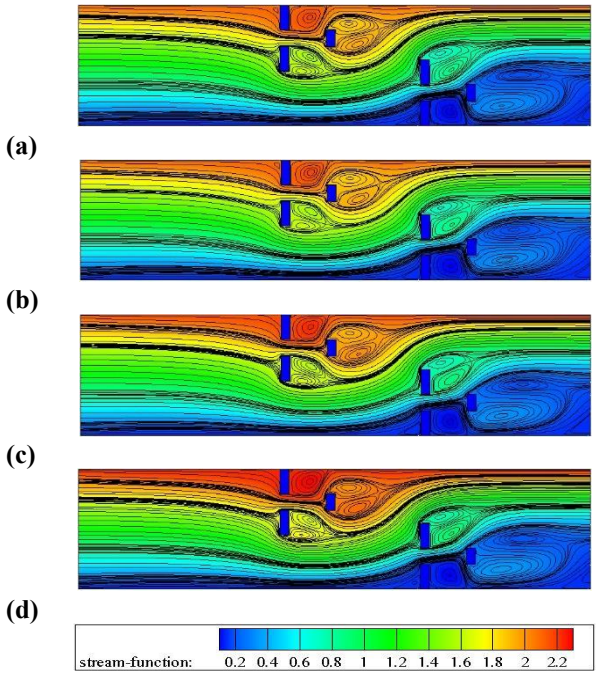

Figure 5. Stream-function field (Ψ in Kg s^{-1}) for ϕ = (a) 0.5%, (b) 1%, (c) 2%, and (d) 4%, $Re = 50\times10^2$

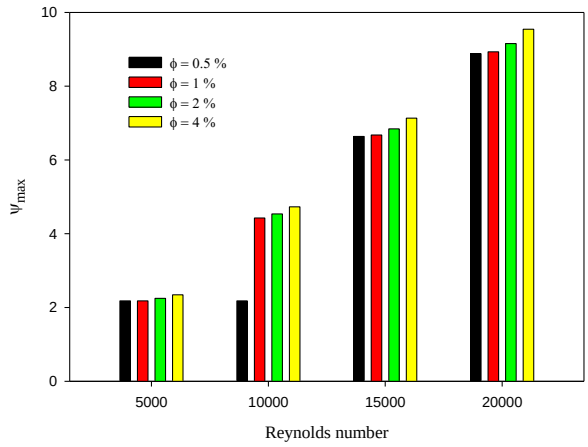

Figure 6. Ψ_{max} for various Re numbers and ϕ concentrations

4.3 Speed field

There are very high mean-velocity (V) values across the gaps between the interior-faces of the intermittent deflectors, due to the high Pd on their left-sides, due to the reduction in the flow-area in this exchanger region (Figure 7).

The V value is also increased in the regions between the top-edges of the intermittent deflectors and the exchanger walls, due to the strong deformation of the nanofluid field, due to the presence of these promoters. While, there are very low speeds behind the intermittent deflectors and disconnected bars, due to low-Pd on their back-sides and as expected, the V augments with the ϕ fraction.

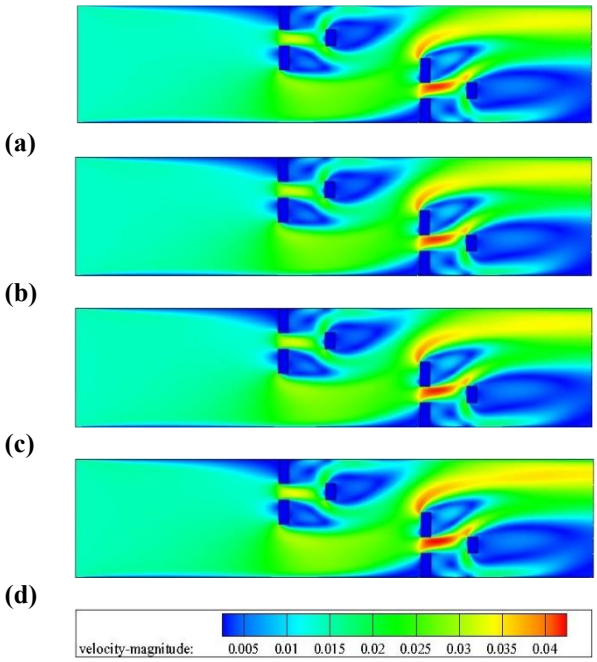

Figure 7. V field (in m s^{-1}) for ϕ = (a) 0.5%, (b) 1%, (c) 2%, and (d) 4%, $Re = 50\times10^2$

The axial-speed values (u) are very low near the intermittent deflectors, especially near their right-sides. This reduction is due to lower Pd values, and the emergence of cells of reverse nanofluid-flows with negative-speeds. These opposite currents constitute recycling-units, where their strength increases with increasing ϕ and Re values, as shown in Figures 8 and 9.

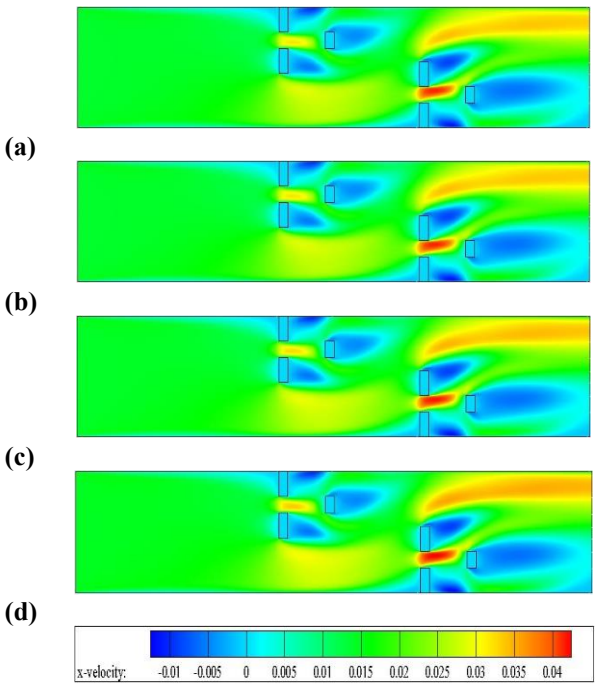

Figure 8. u field (in m s^{-1}) for ϕ = (a) 0.5%, (b) 1%, (c) 2%, and (d) 4%, $Re = 50\times10^2$

The results also show a rise in u values through the last intermittent deflector as well as near its tip to the exchanger outlet, neat its upper wall.

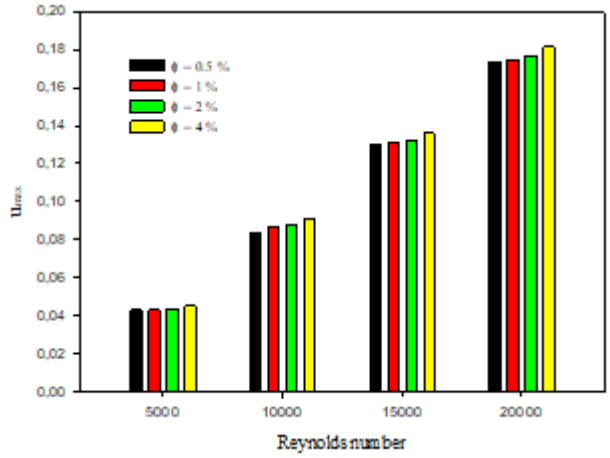

Figure 9. u_{max} for various Re numbers and ϕ concentrations

4.4 K field

The kinetic energy of the turbulence (k) is high next to the sharp-edges of the intermittent deflectors and near their upper-right-sides, as well as, next to the front-sides of the disconnected bars (Figure 10). The k value is improved by increasing the value of Re and by augmenting the Al_2O_3 concentration in the base fluid (H_2O) (Figure 11). This improvement in *k* value is observed on the upper-back of the second intermittent deflector, as well as, near the upper-front-side of the last disconnected bar (Figure 10).

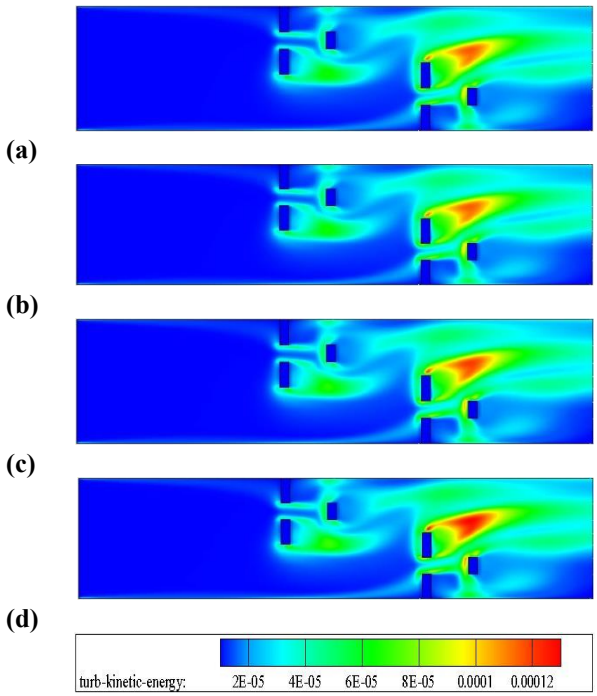

Figure 10. k field (in m^{-2} s^{-2}) for ϕ = (a) 0.5%, (b) 1%, (c) 2%, and (d) 4%, $Re = 50\times10^2$

4.5 μ_t field

In Figure 12, there are high μ_t values (turbulent viscosity) in front and behind the upper part of each intermittent deflector, and on the back-area of the disconnected bars, as well as, at the exchanger exit. While, their values are very low across the gapes, and next to the promoters near the exchanger surfaces,

as well as, adjacent to the top, lower and front sides of each disconnected bar.

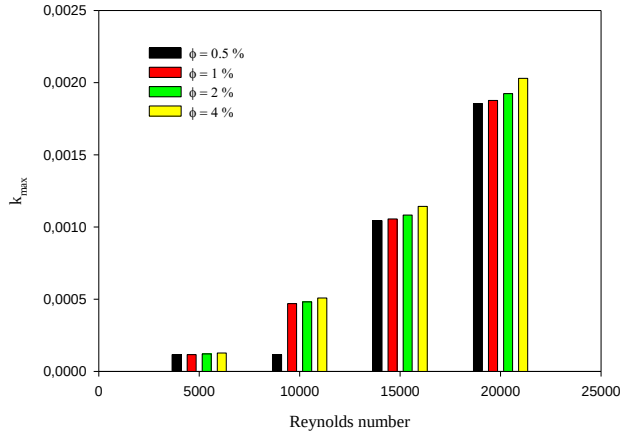

Figure 11. k_{max} for various Re numbers and ϕ concentrations

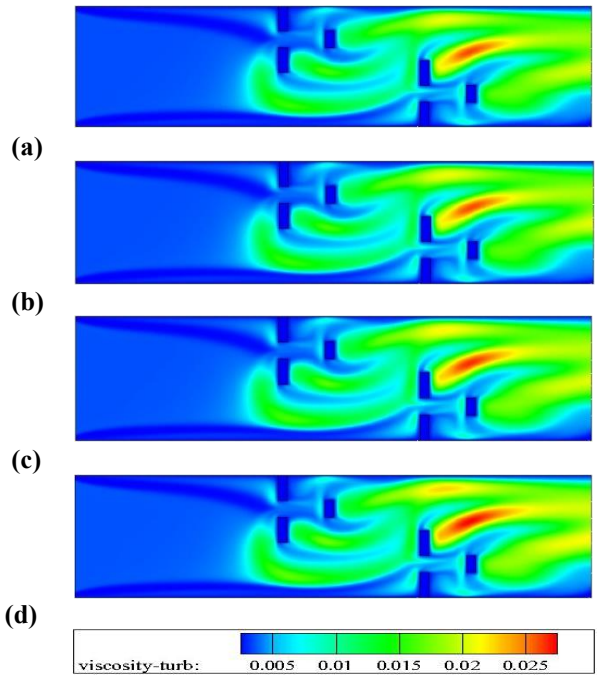

Figure 12. μ_t field (in kg m^{-1} s^{-1}) for ϕ = (a) 0.5%, (b) 1%, (c) 2%, and (d) 4%, $Re = 50\times10^2$

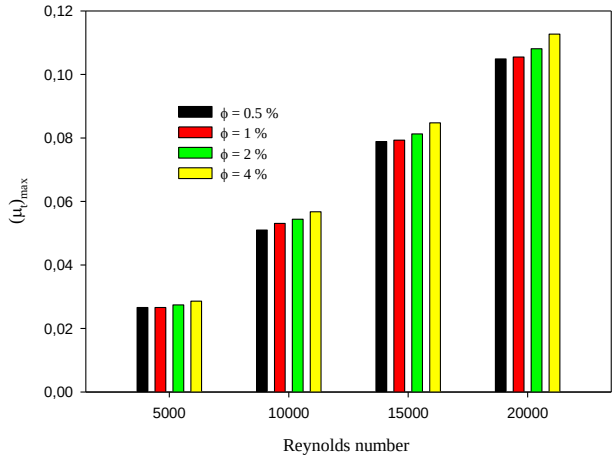

Figure 13. $\mu_{t\,max}$ for various Re numbers and ϕ concentrations

Increasing the concentration (ϕ) of Al_2O_3 solid particles in water with high values of Re number improves μ_t values (Figure 13), especially between the second intermittent deflector and the last disconnected bar on their upper-part (Figure 12).

5. CONCLUSION

The nanofluid dynamics simulation under various Re and ϕ cases in a 2D rectangular-duct Al_2O_3/H_2O-heat exchanger with intermittent deflectors and disconnected bars has been conducted. The discontinuous structure of the deflectors allows reducing the Pd on its front-corner by passing the nanofluid between their internal-surfaces. Also, the field is detached from the front-sharp-edge, forcing the creation of recycling-rings on their back-areas. While, the presence of the disconnected-bar model in both the top and the lower stations of the exchanger allows an improvement in the flow disturbance across the gaps through their interior-surfaces, and the formation of new recycling-cells near their right-sides. The strength of these vortices' cells is improved by improving the nanofluid in larger quantities in terms of the Al_2O_3 particles, and by enhancing the flow field in larger rates in terms of the Reynolds number. Increasing the ϕ concentration of Al_2O_3 in the H_2O with high Re values improves the Pd, Ψ, V, k and μ_t values.

REFERENCES

[1] Ozerinc, S., Kakaç, S., Yazıcıoglu, A.G. (2010). Enhanced thermal conductivity of nanofluids: A state-of-the-art review. Microfluid Nanofluid, 8: 145-170. https://doi.org/10.1007/s10404-009-0524-4

[2] M'hamed, B., Sidik, N.A.C., Yazid, M.N.A.W.M., Mamat, R., Najafi, G., Kefayati, G.H.R. (2016). A review on why researchers apply external magnetic field on nanofluids. International Communications in Heat and Mass Transfer, 78: 60-67. https://doi.org/10.1016/j.icheatmasstransfer.2016.08.023

[3] Liang, G., Mudawar, I. (2019). Review of single-phase and two-phase nanofluid heat transfer in macro-channels and micro-channels. International Journal of Heat and Mass Transfer, 136: 324-354. https://doi.org/10.1016/j.ijheatmasstransfer.2019.02.086

[4] Kakaç, S., Pramuanjaroenkij, A. (2016). Single-phase and two-phase treatments of convective heat transfer enhancement with nanofluids - a state-of-the-art review. International Journal of Thermal Sciences, 100: 75-97. https://doi.org/10.1016/j.ijthermalsci.2015.09.021

[5] Zayed, M.E., Zhao, J., Du, Y., Kabeel, A.E., Shalaby, S.M. (2019). Factors affecting the thermal performance of the flat plate solar collector using nanofluids: A review. Solar Energy, 182: 382-396. https://doi.org/10.1016/j.solener.2019.02.054

[6] Estellé, P., Cabaleiro, D., Żyła, G., Lugo, L., Murshede, S.M.S. (2018). Current trends in surface tension and wetting behavior of nanofluids. Renewable and Sustainable Energy Reviews, 94: 931-944. https://doi.org/10.1016/j.rser.2018.07.006

[7] Farhana, K., Kadirgama, K., Rahman, M.M., Ramasamy, D., Noor, M.M., Najafi, G., Samykano, M., Mahamude,

A.S.F. (2019). Improvement in the performance of solar collectors with nanofluids - A state-of-the-art review. Nano-Structures & Nano-Objects, 18: 100276. https://doi.org/10.1016/j.nanoso.2019.100276

[8] Ahmad, S.H.A., Saidur, R., Mahbubul, I.M., Al-Sulaiman, F.A. (2017). Optical properties of various nanofluids used in solar collector: A review. Renewable and Sustainable Energy Reviews, 73: 1014-1030. https://doi.org/10.1016/j.rser.2017.01.173

[9] Akilu, S., Sharma, K.V., Baheta, A.T., Mamat, R. (2016). A review of thermophysical properties of water based composite nanofluids. Renewable and Sustainable Energy Reviews, 66: 654-678. https://doi.org/10.1016/j.rser.2016.08.036

[10] Menni, Y., Chamkha, A.J., Azzi, A. (2019). Nanofluid flow in complex geometries - A review. Journal of Nanofluids, 8(5): 893-916. https://doi.org/10.1166/jon.2019.1663

[11] Minakov, A.V., Guzei, D.V., Meshkov, K.N., Popov, I.A., Shchelchkov, A.V. (2017). Experimental study of turbulent forced convection of nanofluid in channels with cylindrical and spherical hollows. International Journal of Heat and Mass Transfer, 115: 915-925. https://doi.org/10.1016/j.ijheatmasstransfer.2017.07.117

[12] Mohebbi, R., Rashidi, M.M., Izadi, M., Sidik, N.A.C., Xian, H.W. (2018). Forced convection of nanofluids in an extended surfaces channel using lattice Boltzmann method. International Journal of Heat and Mass Transfer, 117: 1291-1303. https://doi.org/10.1016/j.ijheatmasstransfer.2017.10.063

[13] Selimefendigil, F., Öztop, H.F. (2018). Numerical analysis and ANFIS modeling for mixed convection of CNT-water nanofluid filled branching channel with an annulus and a rotating inner surface at the junction. International Journal of Heat and Mass Transfer, 127: 583-599. https://doi.org/10.1016/j.ijheatmasstransfer.2018.07.038

[14] Xu, H., Cui, J. (2018). Mixed convection flow in a channel with slip in a porous medium saturated with a nanofluid containing both nanoparticles and microorganisms. International Journal of Heat and Mass Transfer, 125: 1043-1053. https://doi.org/10.1016/j.ijheatmasstransfer.2018.04.124

[15] Ameri, M., Eshaghi, M.S. (2018). Exergy and thermal assessment of a Novel system utilizing flat plate collector with the application of nanofluid in porous media at a constant magnetic field. Thermal Science and Engineering Progress, 8: 223-235. https://doi.org/10.1016/j.tsep.2018.08.004

[16] Edalatpour, M., Solano, J.P. (2017). Thermal-hydraulic characteristics and exergy performance in tube-on-sheet flat plate solar collectors: Effects of nanofluids and mixed convection. International Journal of Thermal Sciences, 118: 397-409. https://doi.org/10.1016/j.ijthermalsci.2017.05.004

[17] Tomy, A.M., Ahammed, N., Subathra, M.S.P., Asirvatham, L.G. (2016). Analysing the performance of a flat plate solar collector with silver/water nanofluid using artificial neural network. Procedia Computer Science, 93: 33-40. https://doi.org/10.1016/j.procs.2016.07.178

[18] Anbuchezhian, N., Srinivasan, K., Chandrasekaran, K., Kandasamy, R. (2012). Thermophoresis and Brownian motion effects on boundary layer flow of nanofluid in presence of thermal stratification due to solar energy. Applied Mathematics and Mechanics, 33(6): 765-780. https://doi.org/10.1007/s10483-012-1585-8

[19] Anbuchezhian, N., Srinivasan, K., Chandrasekaran, K., Kandasamy, R. (2013). Magnetohydrodynamic effects on natural convection flow of a nanofluid in the presence of heat source due to solar energy. Meccanica, 48: 307-321. https://doi.org/10.1007/s11012-012-9602-x

[20] Ghorbanian, A., Tahari, M., Hatami, M. (2017). Physical optimization of a wavy porous cavity filled by nanofluids in the presence of solar radiations using the Box-Behnken design (BBD). The European Physical Journal Plus, 132: 278. https://doi.org/10.1140/epjp/i2017-11583-8

[21] Khamis, S., Makinde, D.O., Nkansah-Gyekye, Y. (2015). Unsteady flow of variable viscosity Cu-water and Al_2O_3-water nanofluids in a porous pipe with buoyancy force. International Journal of Numerical Methods for Heat & Fluid Flow, 25(7): 1638-1657. https://doi.org/10.1108/HFF-09-2014-0286

[22] Meibodi, S.S., Kianifar, A., Mahian, O., Wongwises, S. (2016). Second law analysis of a nanofluid-based solar collector using experimental data. Journal of Thermal Analysis and Calorimetry, 126: 617-625. https://doi.org/10.1007/s10973-016-5522-7

[23] Khullar, V., Tyagi, H. (2012). A study on environmental impact of nanofluid based concentrating solar water heating system. International Journal of Environmental Studies, 69(2): 220-232. https://doi.org/10.1080/00207233.2012.663227

[24] Matin, M.H., Hosseini, R. (2014). Solar radiation assisted mixed convection MHD flow of nanofluids over an inclined transparent plate embedded in a porous medium. Journal of Mechanical Science and Technology, 28(9): 3885-3893. https://doi.org/10.1007/s12206-014-0852-5

[25] Menni, Y., Chamkha, A.J., Zidani, C., Benyoucef, B. (2019). Heat and nanofluid transfer through baffled channels in different outlet models. Mathematical Modelling of Engineering Problems, 6(1): 21-28. https://doi.org/10.18280/mmep.060103

[26] Menni, Y., Chamkha, A.J., Zidani, C., Benyoucef, B. (2019). Numerical analysis of heat and nanofluid mass transfer in a channel with detached and attached baffle plates. Mathematical Modelling of Engineering Problems, 6(1): 52-60. https://doi.org/10.18280/mmep.060107

[27] Asadikia, A., Mirjalily, S.A.A., Nasirizadeh, N., Kargarsharifabad, H. (2020). Characterization of thermal and electrical properties of hybrid nanofluids prepared with multi-walled carbon nanotubes and Fe_2O_3 nanoparticles. International Communications in Heat and Mass Transfer, 117: 104603. https://doi.org/10.1016/j.icheatmasstransfer.2020.104603

[28] Balaji, T., Selvam, C., Mohan Lal, D., Harish, S. (2020). Enhanced heat transport behavior of micro channel heat sink with graphene based nanofluids. International Communications in Heat and Mass Transfer, 117: 104716. https://doi.org/10.1016/j.icheatmasstransfer.2020.104716

[29] Suresh, S., Venkitaraj, K.P., Selvakumar, P., Chandrasekar, M. (2011). Synthesis of Al_2O_3-Cu/water

hybrid nanofluids using two step method and its thermo physical properties. Colloids and Surfaces A: Physicochemical and Engineerign Aspects, 388: 41-48. https://doi.org/10.1016/j.colsurfa.2011.08.005

[30] Suresh, S., Venkitaraj, K.P., Selvakumar, P., Chandrasekar, M. (2012). Effect of Al_2O_3-Cu/water hybrid nanofluid in heat transfer. Experimental Thermal and Fluid Science, 38: 54-60. https://doi.org/10.1016/j.expthermflusci.2011.11.007

[31] Baby, T.T., Sundara, R. (2013). Synthesis of silver nanoparticle decorated multiwalled carbon nanotubes-graphene mixture and its heat transfer studies in nanofluid. AIP Advances, 3: 012111. https://doi.org/10.1063/1.4789404

[32] Akilu, S., Baheta, A.T., Sharma, K.V. (2017). Experimental measurements of thermal conductivity and viscosity of ethylene glycol-based hybrid nanofluid with TiO_2-CuO/C inclusions. Journal of Molecular Liquids, 246: 396-405. https://doi.org/10.1016/j.molliq.2017.09.017

[33] Aghabozorg, M.H., Rashidi, A., Mohammadi, S. (2016). Experimental investigation of heat transfer enhancement of Fe_2O_3-CNT/water magnetic nanofluids under laminar, transient and turbulent flow inside a horizontal shell and tube heat exchanger. Experimental Thermal and Fluid Science, 72: 182-189. https://doi.org/10.1016/j.expthermflusci.2015.11.011

[34] Terrones, M. (2003). Science and technology of the twenty-first century: Synthesis, properties, and applications of carbon nanotubes. Annual Review of Materials Research, 33: 419-501. https://doi.org/10.1146/annurev.matsci.33.012802.1002 55

[35] Demartini, L.C., Vielmo, H.A., Möller, S.V. (2004). Numeric and experimental analysis of the turbulent flow through a channel with baffle plates. Joural of the Brazilian Society of Mechanical Sciences and Engineering, 26(2): 153-159. http://dx.doi.org/10.1590/S1678-58782004000200006

[36] Pourfattah, F., Motamedian, M., Sheikhzadeh, G., Toghraie, D., Akbari, O.A. (2017). The numerical investigation of angle of attack of inclined rectangular rib on the turbulent heat transfer of Water-Al_2O_3 nanofluid in a tube. International Journal of Mechanical Sciences 131-132: 1106-1116. http://dx.doi.org/10.1016/j.ijmecsci.2017.07.049

[37] Nasiruddin, Siddiqui, M.H.K. (2007). Heat transfer augmentation in a heat exchanger tube using a baffle. International Journal of Heat and Fluid Flow, 28(2): 318-328. https://doi.org/10.1016/j.ijheatfluidflow.2006.03.020

[38] Patankar, S.V. (1980). Numerical Heat Transfer and Fluid Flow, McGraw-Hill, New York.

[39] Launder, B.E., Spalding, D.B. (1974). The numerical computation of turbulent flows. Computer Methods in Applied Mechanics and Engineering, 3(2): 269-289. https://doi.org/10.1016/0045-7825(74)90029-2

[40] Chamkha, A.J., Menni, Y., Ameur, H. (2020). Thermal-aerodynamic performance measurement of air heat transfer fluid mechanics over s-shaped fins in shell-and-tube heat exchangers. Journal of Applied and Computational Mechanics, 7(2). https://doi.org/10.22055/JACM.2020.32107.1970